Mon. Not. R. astr. Soc. (1978) **182**, 687–704

Studies of bipolar nebulae – V. The general phenomenon

Nuria Calvet and Martin Cohen *Department of Astronomy, University of California, Berkeley, California 94720, USA*

Received 1977 August 22

Summary. Optical spectrophotometry, infrared photometry and radio continuum observations are combined to investigate the class of bipolar nebulae defined purely morphologically. The evolutionary status of these objects is considered. A few represent pre-main sequence objects; most seem to be proto-planetary nebulae; and a small number are evolved planetary nebulae.

1 Introduction

In recent years much attention has been given to a few bipolar nebulae that are extremely bright at infrared wavelengths: HD 44179 (Cohen *et al.* 1975, Paper I); CRL 2688 (Ney *et al.* 1975; Cohen & Kuhi 1977a, Paper II); CRL 618 (Westbrook *et al.* 1975); CRL 2789 (Cohen 1977, Paper III). Bipolar nebulae consist of two, usually symmetrical, lobes with either a visible star and/or an infrared source between the lobes. This paper represents an attempt to investigate the general class of bipolar nebulae, defined purely morphologically, using optical spectroscopy and/or broadband infrared data obtained for ten objects. Some of these objects have been studied by other authors but others are still under-observed. The principal aim of our study is to determine if these nebulae represent a homogeneous group of objects, and if stars of very different mass may appear in such nebulae at different evolutionary phases. The objects discussed individually in this paper are: Lk Hα-233, Lk Hα-208, M2–9, M1–91, CRL 618, NGC 2346, M3–28, Parsamyan 22, M1–99 and Parsamyan 15. Fig. 1 summarizes the nebular structures by means of sketches.

2 The observations

Optical spectroscopy was obtained using the image-tube scanner on the Lick Observatory 3-m reflector. Spectra cover the range λλ 4270–6700 with 7 Å resolution. Infrared photometry was acquired at 1.6, 2.3 and 3.5 μm using the University of Minnesota/University of California at San Diego 1.5-m reflector on Mt Lemmon, Arizona. Some infrared observations at longer wavelengths have already been published for these objects (Cohen 1973a, 1974a). Radio continuum measurements were attempted at 31 and 90 GHz with the NRAO* 11-m

*The NRAO is operated by Associated Universities, Inc., under contract with the National Science Foundation.

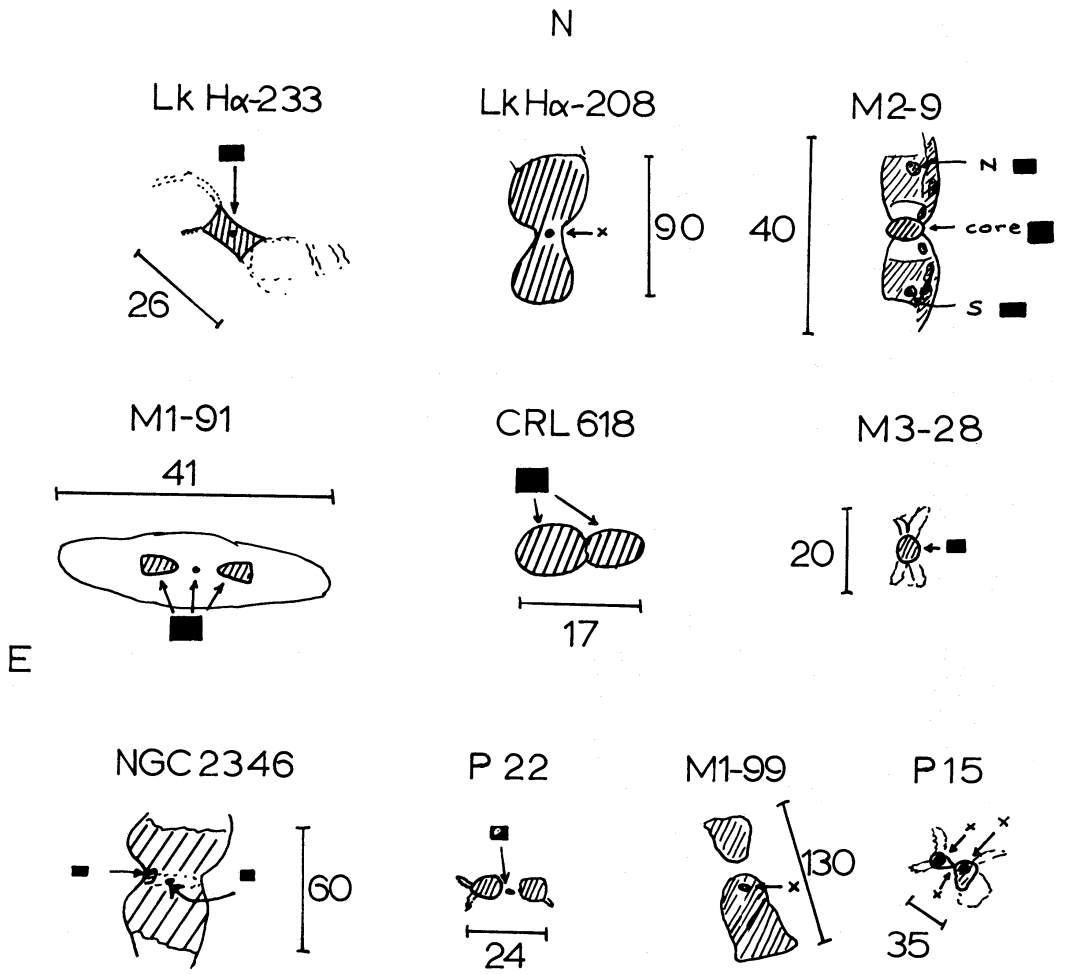

Figure 1. Sketches showing the nebular structure of the ten objects discussed. Scales represent units of arcsec. Apertures used for optical spectroscopy are shown as black rectangles to scale unless they are too small, in which case a cross indicates the region studied.

antenna in Tucson, Arizona. Table 1 summarizes the new infrared photometry and Table 2 the radio observations.

We have observed a grid of about 80 stars of known spectral type using the image-tube scanner on the 3-m telescope. We have extracted the wings of the hydrogen line profiles (Hα, Hβ, Hγ) from these spectra and have measured the depths of various photospheric features (relative to continuum) empirically found to be diagnostic of spectral type. In this way we can attempt spectral classification in our spectral region at low resolution. These

Table 1. Previously unpublished infrared data for bipolar nebulae.

	[1.6]	[2.3]	[3.5]	Beam (arcsec)
M1–91	11.79 ± 0.05	9.34 ± 0.01	6.52 ± 0.01	9
Parsamyan 22	>12.6	11.96 ± 0.24	10.41 ± 0.23	17
M1–99	9.85 ± 0.01	8.60 ± 0.01	6.91 ± 0.01	9
Parsamyan 15E	11.37 ± 0.12	10.69 ± 0.08	9.53 ± 0.20	17
Parsamyan 15W	11.67 ± 0.24	11.69 ± 0.24	>10.7	17
Parsamyan 15 central	11.44 ± 0.18	10.63 ± 0.10	8.94 ± 0.08	17

Upper limits are 3σ of the mean; errors are 1σ of the mean.

Table 2. 31.4-GHz radio observations.

	S (mJy)
Lk Hα-233	<140
Lk Hα-208	<50
M1–91*	<180
NGC 2346	<60
M3–28*	<290
Parsamyan 22	<260
M1–99	10.00 ± 0.16 Jy

*Upper limits are 1σ. Welch & Wright (unpublished) have obtained 1σ upper limits at 23 GHz of 100 mJy for M1–91 and 100 mJy for M3–28 using a two-element interferometer with 6-m antennae.

observations of standard stars also yield intrinsic narrowband continuum indices between 5400 and 6700 Å, and 6000 and 6700 Å (Cohen & Kuhi 1976). These enable us to determine the value of reddening-dependent extinction from the observed continuum colours of an object, once we have classified it.

3 Individual objects

3.1 LK Hα-233

Herbig (1960) first called attention to this nebulous emission-line star that appears to lie within a small dark cloud that includes several other faint emission Hα stars. He pointed out that the bright B1.5 V star HD 213976, with distance modulus 9.6, lies close to the edge of the dark cloud. This suggests that the cloud lies at a distance $\gtrsim 880$ pc. The X-shaped nebulosity that is centred on Lk Hα-233 (*cf.* Herbig (1960), Fig. 13) extends some distance from the star and fades away both to the east and west, arguing for an intimate association between Lk Hα-233 and this cloud.

Three scanner spectra (1974 July, 1975 June and 1976 July) indicate a spectral type of A7 V, and the continuum indices suggest an A_V of 2.56. We have examined our spectra of Lk Hα-231 and 232, which lie in the same dark cloud. We find types of K4 V and K3 V, with A_V of 2.35 and 2.44, respectively. This close agreement for all three stars argues that this extinction arises within the interstellar medium. Lk Hα-231 and 232 have emission-line spectra with strong Hα and He I, which suggest that they are very young objects and are likely to be over-luminous for their spectral types. L Hα-35 in NGC 2264 is of type K4 V, according to our data, and has a spectrum very similar to those of Lk Hα-231 and 232. L Hα-35 is over-luminous in V by ~2 mag (Herbig 1954). If Lk Hα-231 and 232 were over-luminous by about this amount their distances would be 700 and 600 pc, respectively. From Fitzgerald (1968) we find that a distance of ~1 kpc is necessary to produce an interstellar extinction of 2.5 mag in this direction. Therefore, we shall adopt a distance of 880 pc to Lk Hα-233.

After correction for 2.56 mag of extinction we have constructed the energy distribution of Lk Hα-233 between 0.43 and 18 μm (*cf.* Cohen 1974a). Since we have established that none of this extinction is likely to arise in the circumstellar shell of Lk Hα-233, it is valid to de-redden the infrared fluxes by an amount corresponding to this A_V. The de-reddened optical fluxes between 0.43 and 0.67 μm have been extrapolated using a blackbody curve appropriate to the effective temperature of an A7 V, to assess the stellar contribution to the overall energy distribution. If we assume that the integrated flux over all wavelengths from

Lk Hα-233 is the same in all directions, then this assumption of isotropic radiation enables the derivation of luminosities from integrated fluxes. We find the stellar (blackbody) luminosity to be $28D^2L_\odot$, and the infrared contribution (the excess over stellar flux from 1.6 μm to ∞ using the method of Cohen (1973b)) to be $\geqslant 128D^2L_\odot$, where D is the distance in kpc. Thus a lower limit to L_{bol} for Lk Hα-233 is $121L_\odot$.

We have made an estimate of the weak Hβ emission that seems to be present within the photospheric absorption feature in 1975 June, by comparison with the Hβ profiles of standard stars. Similarly, any emission at Hγ is extremely weak. We have corrected our estimate of the observed Balmer decrement for an extinction of 2.56 mag and have then located Lk Hα-233 in the diagram due to Gerola, Salem & Panagia (1971). These authors computed the Balmer decrement for a nebula as a function of the ratio of collisional ionization to total ionization, varying N_e and the size of the nebula. Lk Hα-233 cannot be located precisely within this diagram on the basis of our data. However, its general location seems to suggest that the ionization is produced completely by collisions, and that the nebula is compact and of high density. The agreement between the extinctions for Lk Hα-231, 232 and 233 argues that in Lk Hα-233 the optical continuum is entirely photospheric in origin. This implies that any continuum from the zone in which the emission lines arise must be much smaller than the stellar continuum. This too suggests a zone small in comparison with the stellar radius. We notice that the intensity of Hα emission, relative to continuum, has been increasing monotonically in Lk Hα-233 since 1974. Similarly the strength of the red doublet of [S II] increased between 1974 and 1975, although unfortunately we did not include these lines in our 1976 spectrum. The ratio of [S II] lines indicates a density $N_e = 2500\,\mathrm{cm}^{-3}$, suggesting that these lines are formed outside the central zone of high density.

Since the region of ionization is very small, the illumination of the extended nebula around Lk Hα-233 must be due to scattering of light from the central zone by dust particles. Taking a scattering optical depth at V of ~ 5 we can compute the number of scattering particles in the nebula required to produce the almost uniform brightness seen with the TV system at the 3-m telescope. For reasonable dielectric grains (e.g. silicates, ices) of radius $\sim 0.05\,\mu$m, the mass of scattering grains in the nebula is $\sim 0.03 M_\odot$. The hottest grains that seem to be present have temperature ~ 1300 K (from the shape of the excess infrared energy distribution) and if these were blackbody grains their distance from the star would be $\sim 4 \times 10^{12}$ cm.

3.2 LK Hα-208

This star lies in the centre of the classical biconical nebula, well shown in Herbig's (1960, Fig. 8) photograph, and the geometry argues strongly for a central disk of material. Our scanner criteria for spectral classification indicate an F0 V, and the continuum indices show $A_V = 0.35$. We have also obtained a spectrum of Lk Hα-209 which appears to lie in the same dark cloud as Lk Hα-208 (Herbig 1960). We have classified Lk Hα-209 as a G3 V star from which we have determined $A_V = 0.26$. It would appear that the interstellar reddening towards Lk Hα-208 and 209 produces this extinction of ~ 0.3 mag. We have re-reddened the optical and infrared data (Cohen 1973a) according to this quantity and have fitted a blackbody of $T_{eff} = 7000$ K to the resulting optical energy distribution to estimate the stellar contribution to the bolometric luminosity. The components of luminosity are $14.3D^2L_\odot$ (L^*) and $89D^2L_\odot$ (from 1.6 μm to ∞), where D is the distance in kpc.

The bright A0 star HD 41787 ($V = 8.9$) lies 3 arcmin east of Lk Hα-208. Assuming that this star has luminosity class V yields a lower limit on the distance of the dark cloud in which Lk Hα-208 lies. This is $D \geqslant 0.44$ kpc. Consequently, $L_{bol} \geqslant 20L_\odot$ for Lk Hα-208.

Lk Hα-208 shows moderate emission at Hα and we have estimated the very weak emission at Hβ and Hγ by comparing the line profiles of this star with those of an F0 V standard. The estimated Balmer decrement suggests that the ionization is produced entirely by collisions in a dense envelope of great extent – *cf.* Gerola *et al.* (1971, Fig. 1). No other emission lines are seen in our spectral region that could be used to make an estimate of the nebular mass.

Herbig (1960) cites the spectral type of Lk Hα-208 as B1 according to Hubble, but argues himself for an underlying late B star with some shell emission. There would appear to be some evidence for a systematic trend in the type of Lk Hα-208 from early B in 1922 to F0 at the present, although the data are not compelling since different spectral regions and criteria for classification have been used. The hottest grains that may be seen in the infrared spectrum of Lk Hα-208 have $T \sim 1600$ K so the inner edge of the dust distribution is $\sim 2 \times 10^{12}$ cm from the stellar surface.

3.3 M2–9

This highly symmetrical nebula was first found to be a near-infrared source by Allen & Swings (1972), who also discussed the spectrum of the central condensation and the extended nebula. We have obtained spectra of the central condensation and of the brightest nebulous knots in each of the north and south wings (Fig. 1). The spectra (Fig. 2) are dominated by strong Balmer lines, and contain strong lines of [O III], [He I] and [O I], as well as weaker lines of [S III], Si II, [N I], [N II], [Fe II] and [Fe III]. A continuum is also present in each location.

We have determined the extinction towards these three regions using the Balmer decrements and the work of Capriotti (1964), and have corrected other emission-line intensities using these values of A_V. The values of N_e and T_e that result from the ratios of [N II], [O III] and [O I] lines are summarized in Table 3, along with the excitation class, determined from [O III] and Hβ, as defined by Aller & Liller (1968). A comparison of N_e and T_e derived for [O III], [N II] and [O I] in the centre of M2–9 strongly argues for a stratification of ionization, from a dense [O III] core out to a less dense [O I] zone. By contrast, the conditions in the lobes are suggestive of a very different structure since [O I] densities greatly exceed those for [N II]. This phenomenon could arise from the presence of dense neutral condensations ($N_e \sim 5 \times 10^6$ cm^{-3}) with neutral oxygen and neutral hydrogen cores, immersed in a general, less dense medium ($N_e \sim 10^4$ cm^{-3}).

The Balmer decrement and densities in the lobes of M2–9 indicate that the effects of Balmer self-absorption are small. We are able to predict the observed levels of nebular continuum in the lobes from the observed hydrogen lines, including free–free, bound–free and two-photon emission of purely radiatively ionized hydrogen, with mean conditions of $N_e = 10^4$ cm^{-3} and $T_e = 10^4$ K. However, in the very dense centre of M2–9 the effects of self-absorption become important and we have not attempted to predict the continuum.

Radio continuum observations of M2–9 show that the core emission is dominated by a very compact, high density region, whereas in the lobes, where there are no compact sources, one sees evidence of condensations (Purton, Feldman & Marsh 1975; Marsh, Purton & Feldman 1976).

We have obtained spectropolarimetry of M2–9 using the Lick image-tube scanner with a 4 x 4 arcsec aperture on the central core. Fig. 3 presents this data in the form of plots of the degree of linear polarization and the position angle of the electric vector. We can detect no statistically significant difference between the polarization of the continuum and that of the emission lines. Therefore, we have plotted one point to represent each 200 Å region from

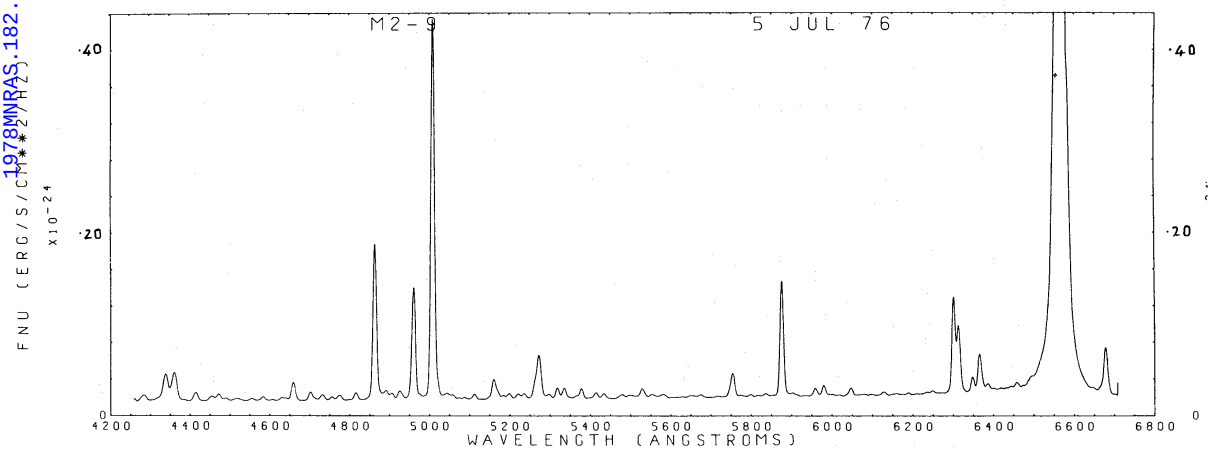

(a)

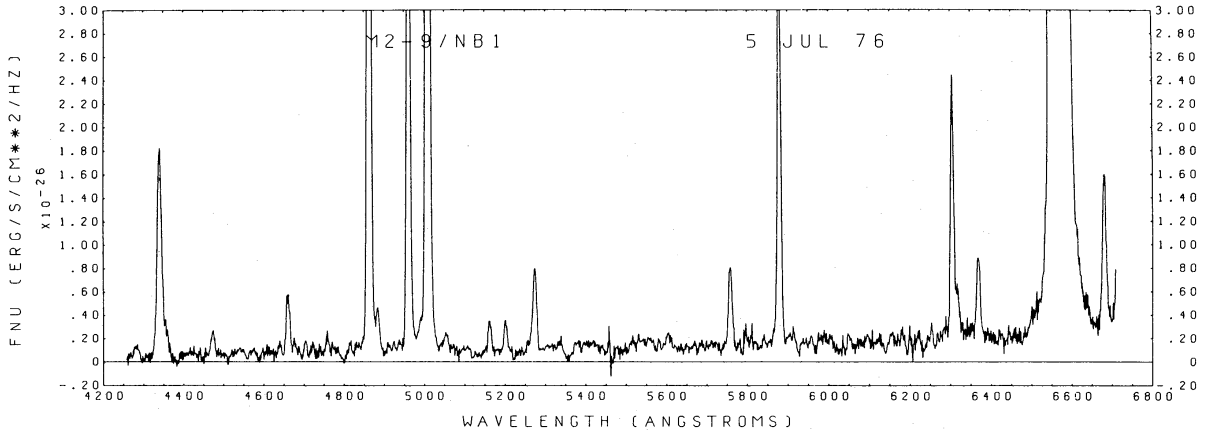

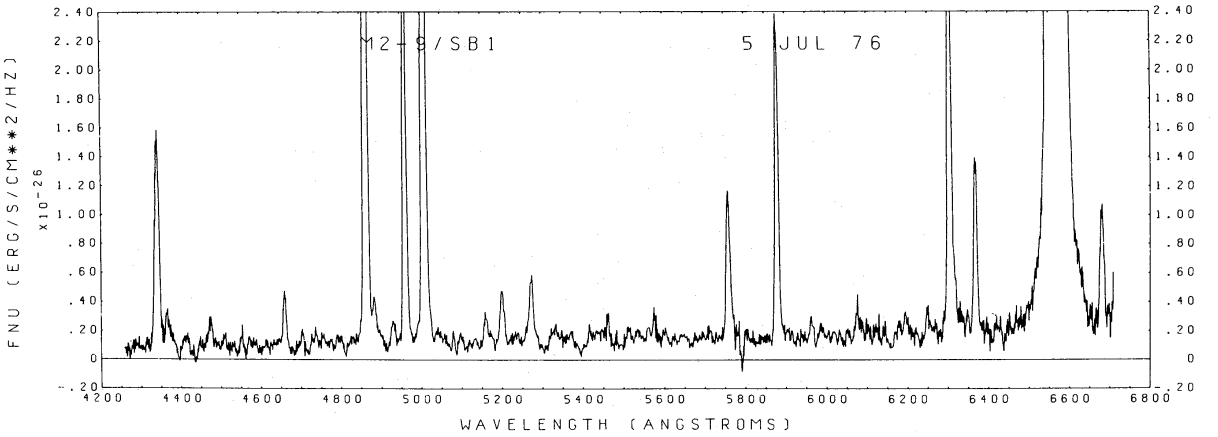

(b)

Figure 2. Spectrophotometry of the central portion of M2–9 obtained with a 4 × 4 arcsec aperture, and of two nebular condensations obtained with 4 × 2.7 arcsec apertures.

our data in order to reduce the noise. There appears to be a very flat portion of the $p(\lambda)$ curve longward of about 5400 Å, whereas the polarization increases quite steeply into the blue. It is tempting to ascribe the increase of polarization in the blue to scattering by very small particles. Following the method described by Cohen & Kuhi (1977b), using $A_V = 5.35$ to represent the extinction (*cf.* Table 3), we find evidence for an extra, polarized

Table 3. Summary of parameters for M2–9.

	Centre		N knot	S knot
T_e (K)	10^4	2×10^4	10^4	10^4
N_e ([O III]) cm^{-3}	10^7	4×10^6		
N_e ([N II]) cm^{-3}	2×10^6	2×10^5	2×10^3	4×10^4
N_e ([O I]) cm^{-3}	2×10^6	3×10^5	4×10^5	2×10^6
Excitation class	3		3	3
A_V (Balmer)	5.35 ± 0.30		2.67 ± 0.14	2.77 ± 0.09

continuum of the form $I'(p) \propto \lambda^{-\alpha}$, where $\alpha = 3.6 \pm 4.2$. The flat polarization could be produced by scattering from either electrons or dust particles. It is surprising to detect *any* polarization given the apparently spherical nature of the core of M2–9. The interstellar polarization in this direction and at the likely distance of M2–9 (see below) contributes only about 0.05 per cent in position angle 140° (Serkowski, Mathewson & Ford 1975). Therefore, the polarization is intrinsic to M2–9, and both p and θ are little altered by this interstellar component ($\Delta p \sim 0.4$ per cent, $\Delta\theta \sim 2°$). However, there is no apparent asymmetry visible in photographs of M2–9 (*cf.* Allen & Swings (1972); van den Bergh 1974) that would suggest that position angle 65° is significant to the nebular structure.

Using the formulation of Kazès, Le Squéren & Gadéa (1975), we can relate the radio flux, the excitation parameter and M_V of the exciting star of M2–9. We find the best match to occur for a B1 star, based upon the radio flux measured by Purton *et al.* (1975). This result is not particularly sensitive to the fact that the radio spectrum of M2–9 is not optically thin. Virtually all the observed luminosity of M2–9 is seen beyond 1.6 μm (Cohen & Barlow 1974). This luminosity is $\geqslant 844 D^2 L_\odot$ where D is the distance in kpc (assuming isotropic radiation). The minimum requirement would be a B1 V star which has a luminosity of $8800 L_\odot$ from which $D \leqslant 3$ kpc. The galactic latitude of M2–9 is +18° which precludes a distance as large as 3 kpc since the distance from the galactic plane would be excessive for an object of either population I or the intermediate population. The fact that the knots are ionized suggests that the exciting star is capable of ionizing the full extent of the nebula.

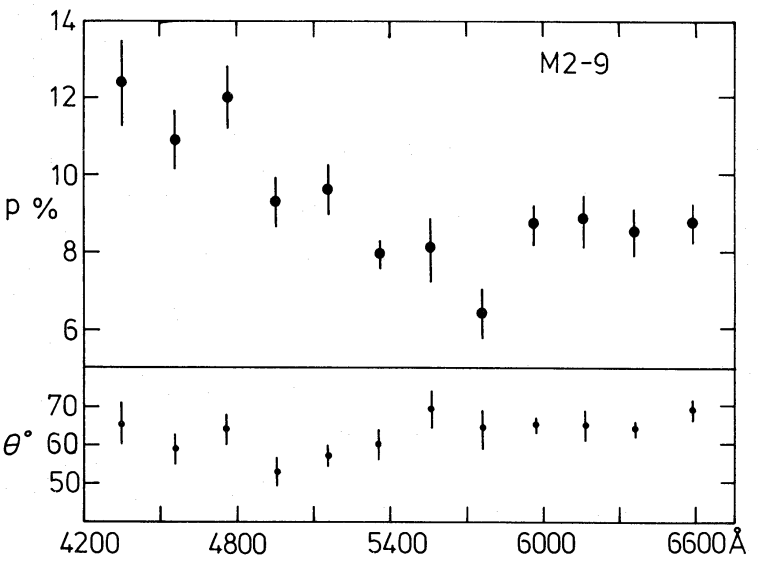

Figure 3. Spectropolarimetry of the centre of M2–9 obtained with a 4 × 4 arcsec aperture, showing the degree of linear polarization and position angle of the electric vector. One point is plotted for each 200 Å interval and error bars represent one standard deviation of the mean.

This would require the radius of the Stromgren sphere around the B1 star to exceed 20 arcsec. For a mean density $N_e \sim 10^3\,cm^{-3}$ (Purton *et al.* 1975), this radius is ~ 0.1 pc. Hence, $D \leqslant 1$ kpc. At such a distance the luminosity and temperature of M2–9 would place it at the beginning of the sequence of nuclei of planetary nebulae (*cf.* Osterbrock 1974). We estimate the total nebular mass of M2–9 to be $\sim 0.2 D^3 M_\odot$ (D in kpc) for a mean core density of $10^6\,cm^{-3}$ and mean density of $10^3\,cm^{-3}$ in the wings. The distance would be of order 0.9 kpc to produce the conventional shell mass of a planetary nebula. The corresponding z distance is ~ 260 pc, quite consistent with an interpretation of M2–9 as a planetary nebula. The location of M2–9 at the beginning of the sequence of nuclei of planetaries, the high density in the core, and the unusual structure of the nebula, all suggest that M2–9 is an object which has recently begun to evolve into a planetary nebula. Such a system would be expected to produce significant expansion velocities. We note that the lobes of M2–9 have radial velocities of ± 15 km/s relative to the core (Allen & Swings 1972). This could represent evidence for an expansion along the north–south axis. There is an alternative explanation in which M2–9 would be a flattened gas disk viewed edge-on, and rotating about an east–west axis. Unfortunately there is no way to distinguish between these two models with the present data.

The structure of M2–9 changed markedly between 1952 and 1971 (Allen & Swings 1972), while the structure of the brightest knots changed in only 2 yr (van den Bergh 1974). We follow these authors in treating these structural changes as due to geometrical variations in the ionizing radiation escaping from the embedded star. The hottest dust grains present around the star have temperature ~ 800 K. For blackbody grains near a B1 star this temperature corresponds to a distance 6×10^{14} cm from the star. If we demand that a beam of ionizing radiation crossed the lobes of M2–9 between 1952 and 1971, the angular velocity of this beam is $\sim 10^{-9}$ rad/s. This corresponds to a velocity of only ~ 5 km/s if the motions of hot dust clouds produce irregular irradiation of the lobes. The 2-yr timescale for changes in the brightness of knots could arise simply from recombination, if $N_e \sim 10^5\,cm^{-3}$. It is possible that 'holes' in the distribution of dust clouds are responsible for the asymmetry that produces the polarization in position angle 65°. One might, therefore, expect to detect changes in this position angle corresponding to motions of the dust clouds on a timescale of ~ 10 yr.

3.4 M1–91

This nebula consists of two highly symmetrical, separated, conical lobes, with a centrally located very faint nucleus. There appears to be a much more extensive halo surrounding this inner structure on deep photographs. We have obtained spectra of the central star and the two bright lobes, infrared observations of the nucleus, and radio upper limits for the whole nebula.

We have determined the extinction from the Balmer decrement in the three regions, assuming a pure recombination spectrum. These extinctions were then used to determine electron densities and temperatures for the regions that produce [O III], [O I], [N II], [N I]. These numbers are summarized in Table 4, which also includes the excitation class, calculated from the ratio [O III]/Hβ.

As for M2–9, conditions around the central star of M1–91 indicate the presence of a stratified ionization structure. In the lobes of M1–91, the more highly ionized species seem to arise in a hotter medium than does the [O I] emission. This suggests the presence of neutral condensations in the lobes. The density of these condensations is indeterminate due to the absence of λ 5577 of [O I].

Table 4. Summary of parameters for M1–91.

	Central star		E lobe	W lobe
T_e (K)	10^4	2×10^4	1.5×10^4	1.5×10^4
N_e ([O III]) cm^{-3}	5×10^6	1.3×10^6	2×10^5	1.4×10^5
N_e ([N II]) cm^{-3}	10^6	4×10^5	8×10^4	6×10^4
T_e ([O I]) K	$<1.5\times10^4$		$<1.2\times10^4$	$<1.3\times10^4$
Excitation class	3.5		3	3

Each of our spectra also indicates the presence of a weak continuum. The nebular continua in the lobes of M1–91 are predictable from the observed hydrogen lines exactly as for M2–9. Mean conditions of $N_e = 10^5\,\mathrm{cm}^{-3}$ and $T_e = 15\,000\,\mathrm{K}$ represent these continua satisfactorily. The centre of M1–91 also shows strong effects of Balmer self-absorption and we shall not discuss the continuum there.

The large Hα halo of M1–91 (seen on the Sky Survey red photograph) suggests that this entire nebula is ionized. We may determine approximate values for N_H, the mean hydrogen density; the distance of M1–91, D kpc; and the temperature of the nucleus (as measured by r_1, *cf.* Osterbrock 1974, Table 2.3), subject to the following assumptions: that the nucleus is capable of ionizing the entire visible nebula, so that $N_H = N_p$ and $N_H^{2/3} D \leqslant 10 r_1$; that the radio flux due to optically thin free–free emission is of order 50 mJy (consistent with our upper limits), from which $N_H^2 D = 8.18\times10^5$; and that we are observing a protoplanetary nebula, the mass of whose shell is $0.17 M_\odot$, hence $N_H D^3 = 1.48\times10^4$. Thus, we find $N_H = 500\,\mathrm{cm}^{-3}$, $D = 3.1$ kpc, $r_1 \geqslant 20$, $T^* \geqslant 30\,000$ K which implies that the star is at least a B0.

This density is so much lower than the densities derived for the forbidden line regions that it is clear that large density gradients are required. M1–91 appears to have an extensive low density ($N_H \sim 500\,\mathrm{cm}^{-3}$) halo, in which most of the nebular continuum arises. Embedded within this halo are denser regions ($\sim 10^5$–$10^6\,\mathrm{cm}^{-3}$) where the bulk of the Balmer line emission is produced. If we calculate the radio flux expected from the lobes of M1–91 on the basis of the emission at Hβ, then we expect ~ 750 mJy from each lobe. However, using the expression for optical depth (Osterbrock 1974)

$$\tau(\mathrm{radio}) = 8.24\times10^{-2} T_e^{-1.35} \nu^{-2.1} N_e^2 L,$$

with $\nu = 31.4$ GHz, $T_e = 10^4$ K, $L = 0.022$ pc (3 arcsec), we find $\tau \sim 1$ when $N_e \sim 4\times10^5\,\mathrm{cm}^{-3}$. Consequently, the inner portions of the nebula are optically thick at $\lambda \sim 1$ cm.

The near-infrared energy distribution is consistent with thermal emission from dust grains at temperature $T \lesssim 1100$ K. The bolometric luminosity of M1–91 is $\geqslant 450 L_\odot$, using our optical and infrared data, hence M1–91 lies at $\log L/L_\odot = 2.65$, $\log T^* = 4.48$, at the beginning of the Harman–Seaton sequence of the nuclei of planetary nebulae. At the distance of 3.1 kpc, M1–91 is ~ 270 pc above the plane. Therefore, all these parameters for M1–91 would be consistent with its being a protoplanetary nebula.

3.5 CRL 618

This bright infrared source has been studied in great detail by Westbrook *et al.* (1975). Their spectra of the brighter nebulous lobe were obtained with 30 Å resolution. Our spectra (Fig. 4) show all the lines listed by Westbrook *et al.* in our spectral region, and establish the great strength of [Fe II] (*cf.* Table 5). A small number of lines in the red apparently are due to permitted Fe II, although the absence of the commonly seen strong multiplets in the

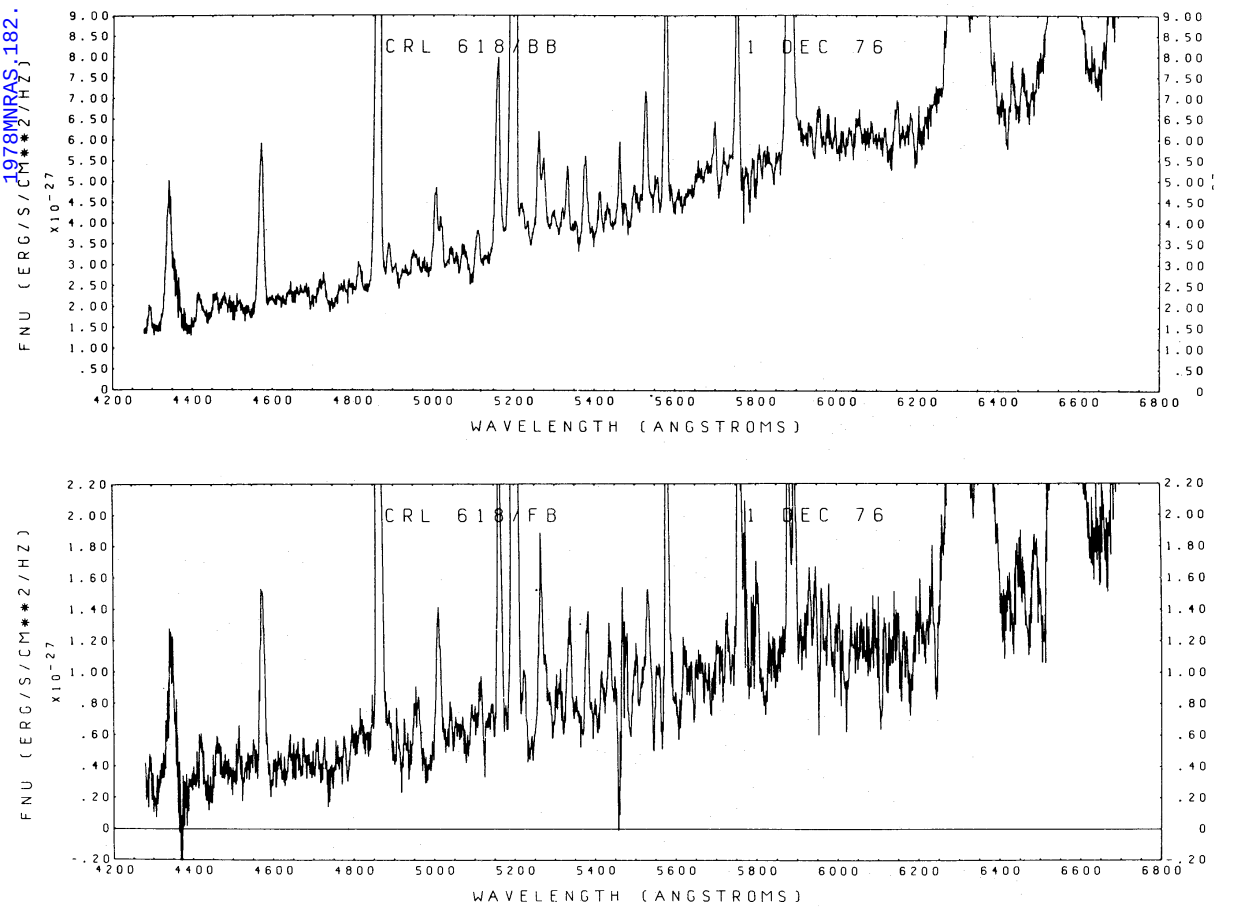

Figure 4. Spectrophotometry of the bright (BB) and faint (FB) lobes of CRL618 obtained with 4 × 2.7 arcsec apertures.

yellow region is puzzling. The great strength of Mg I λ4571 may argue for the existence of cool condensations (*cf.* Aller *et al.* 1972).

The Balmer decrement for the two lobes, assuming that the spectra are produced by photoionization followed by recombination, gives $A_V = 3.45 \pm 0.20$ (bright), $A_V = 4.84 \pm 0.52$ (faint lobe). This is in good agreement with the adopted value of $A_V = 3.5$ for the bright lobe by Westbrook *et al.* We have corrected our fluxes of forbidden emission lines by these values of A_V and we find $T_e = 10^4$ K, $N_e \sim 2 \times 10^5$ cm^{-3} for both lobes. Fig. 4 shows the presence of a strong, steeply rising continuum in each lobe. The nebula continuum due to free–free, bound–free and two-photon emission of hydrogen is far too weak to explain the continuum in either lobe. Consequently CRL618 must be dominantly a reflection nebula surrounding a hot central star (in accord with the optical polarimetry by Westbrook *et al.*). The excitation class derived for both lobes from [O III]/Hβ is 2, suggesting that a very low excitation ionized region surrounds the star. We have computed Zanstra temperatures for the lobes of CRL618 using the ratio of Hβ fluxes to the continua at λ4861. We have made allowance for the difference between theoretical atmospheres and simple blackbody models by recalibrating the temperature scale using Panagia's (1973) computations of the number of Lyman continuum photons. We find 29 800 K for the bright lobe and 30 500 K for the faint lobe. This suggests that the central star is of type B0 V, in agreement with the conclusion of Westbrook *et al.*, and consistent with the absence of He II λ4686 emission.

The shape of the continuum in each lobe corresponds to an extinction for a B0 V star of $A_V = 3.7$ (bright) and 4.2 (faint lobe). Using the intrinsic Hβ flux it is possible to make a

Table 5. Emission lines seen in the bright (B) or faint (F) lobe of CRL 618.

Line	Identification	Lobe	Line	Identification	Lobe
4297	Fe II 28	BF	5413	Fe II 17F	BF
4340	Hγ	BF	5433	Fe II 18F	BF
4414, 16	Fe II 6F	BF	5496	Fe II 17F	BF
4458	Fe II 6F	BF	5527	Fe II 17F	BF
4515	Fe II 6F	F	5556	Fe II 18F	BF
4571	Mg I 1	BF	5577	O I 3F	BF
4640	Fe II 4F	B	5655	Fe II 17F	BF
4815	Fe II 20F	BF	5721	Fe II 33F	BF
4861	Hβ	BF	5741	Fe II 33F	BF
4890	Fe II 4F	BF	5755	N II 3F	BF
4905	Fe II 20F	BF	5809	Fe II 33F	BF
4951	Fe II 20F	BF	5876	He I 11	BF
4959	O III 1F	BF	5895	Na I 1	BF
5007	O III 1F Fe II 20F	BF	5991	Fe II 46	BF
			6084	Fe II 46	BF
5020	Fe II 20F	B	6113	Fe II 46	B
5044	Fe II 20F, 19F	BF	6148	Fe II 74, 46	B
5076	Fe II 19F, 20F	B	6246	Fe II 74	BF
5110	Fe II 18F, 19F	BF	6300	O I 1F	BF
5158	Fe II 18F, 19F	BF	6363	O I 1F	BF
5200	N I 1F	BF	6433	Fe II 40	B
5220	Fe II 19F	BF	6456	Fe II 74	B(F?)
5262	Fe II 19F	BF	6516	Fe II 40	B
5269	Fe II 18F	BF	6548	N II 1F	BF
5300	Fe II 17F, 19F	BF	6563	Hα	BF
5334	Fe II 19F	BF	6584	N II 1F	BF
5348	Fe II 18F	BF	6678	He I 46	BF
5376	Fe II 19F	BF			

prediction of the radio free–free emission, assuming that there is a compact ionized zone surrounding the central star, in which both Hβ emission and radio continuum emission arise. We shall further assume that the nebulous lobes merely reflect the Hβ emission from the central zone. A lower limit to the Hβ flux can be estimated using the observed flux of Westbrook *et al.* for the bright lobe (with an aperture exceeding ours) together with our observed Hβ flux for the faint lobe. We have corrected the observed to intrinsic fluxes using $A_V = 3.5$ (bright) and 4.8 (faint lobe). Assuming that the region is optically thin we predict a radio flux $\geqslant 280$ mJy at 31.4 GHz.

3.6 NGC 2346

This nebula is of interest because the apparent central star is too cool to ionize the object. On the basis of the infrared energy distribution, Cohen & Barlow (1975) suggested that NGC 2346 might be a biconical cometary nebula surrounding a young star. Our spectral classification of the bright central star is A0 III, in agreement with Kohoutek & Senkbeil (1973). However, the presence of He II λ4686 in emission is now well established in this object (Chopinet & Lortet-Zuckermann 1976; Kaler, Aller & Czyzak 1976; Sabbadin 1976). This high excitation suggests that NGC 2346 is a planetary nebula whose true exciting star is as yet unrecognized, as suggested first by Kohoutek & Senkbeil. A short exposure photograph by Minkowski (*cf.* Cohen & Barlow 1975) shows the presence of a luminous condensation a few arcsec east of the obvious central star. We have obtained a spectrum of this

condensation in order to determine its source of excitation, and to see if it contains the exciting star. Its spectrum is quite similar to the general nebular spectrum of NGC 2346 (Kaler *et al.* 1976). The Balmer decrement in the condensation suggests an A_V of 1.53 which we have used to correct the other emission line data to intrinsic fluxes. The condensation has excitation class ~ 5.5, based on both [O III] and He II. From the ratios of [N II] and [O III] lines we find $T_e = 7500$ K and $N_e = 2.5 \times 10^4$ cm^{-3}, making the condensation cooler and denser than the general nebulosity.

The Zanstra temperature (from He II λ4686 and Hβ) of the nebulosity near the A0 star is 95 000 K, using the photographic data of Kaler *et al.*, and 101 000 K using Sabbadin's (1976) data. The photoelectric data of Kaler *et al.* which refer to the entire nebula, and our data for the condensation, yield $T_z = 65\,000$ K. This information strongly suggests that the nucleus of NGC 2346 is indeed an unresolved binary with an unseen very hot component. Broadband ultraviolet observations of the nucleus by the ANS group (Pottasch 1977, private communication) do not reveal anything but the expected flux from the A0 star. Adopting temperatures of 9600 K for the A0 III and 100 000 K for the hotter star, the ultraviolet data constrain the radius of the hotter star to be $\ll 0.1 R_\odot$. The values $\log T^* = 5.00$ and $\log R^*/R_\odot \sim -1.5$ are consistent with the nucleus of a planetary nebula with luminosity $\sim 90 L_\odot$ (O'Dell 1963). If the total mass of the observed nebula is $\sim 0.17 M_\odot$ the mean nebular density is ~ 170 cm^{-3}, and this density implies that the hot degenerate star would be capable of ionizing the entire visible nebula.

The photometry of the A0 III star by Kohoutek & Senkbeil indicates $A_V = 0.62$ and thus the distance to NGC 2346 is 1.7 kpc. One would expect an interstellar extinction of ~ 0.9 mag at this distance, in this longitude (Fitzgerald 1968). It does not appear that the A0 star suffers any appreciable circumstellar reddening. At this distance, the infrared luminosity (Cohen & Barlow 1975) is $\sim 42 L_\odot$ whereas the degenerate star has $L_{bol} \sim 90 L_\odot$. This luminosity, and the infrared energy distribution, are entirely consistent with thermal emission by hot ($T \leqslant 1300$ K) dust grains surrounding the degenerate star. This dust selectively absorbs the He^+ ionizing photons from the hotter star.

The significantly larger value of A_V towards the condensation than that towards the A0 star suggests that the condensation is dustier than the general nebulosity of NGC 2346. The condensation produces a weak optical continuum, roughly half of which can be due to free–free, bound–free and two-photon emission of hydrogen, and it seems to be excited entirely from without. The remaining continuum is consistent with its being light from the A0 star reflected by dust in the condensation and suffering ~ 0.6 mag of extinction.

3.7 M3–28

This very faint nebula consists of an inner elliptical core with tenuous biconical extensions (*cf.* Perek & Kohoutek 1967), rather like the central portions of M2–9. Our spectrum is of this inner core and shows extremely strong red lines of [N II] and blue lines of [O III], with appreciable Balmer and [O I] emission lines. He II λ4686 is weakly present in emission. The Balmer decrement yields $A_V = 5.75 \pm 0.36$ and we have corrected the intensities of other emission lines to obtain the parameters listed in Table 6. There is a great difference between N_e as deduced from [O I] and from [N II], suggesting the existence of dense neutral condensations.

M3–28 is a nebula of very high excitation, based upon both [O III] and He II (*cf.* Table 6). The stellar temperature is 90 000 K, from the ratio of He II λ4686 to Hβ. We can make an estimate of the distance to M3–28 by requiring that the nucleus is capable of fully ionizing the observed nebula. The determination of the Stromgren radius for a star of temperature

Table 6. Parameters of M3–28.

T_e (K)	10^4
N_e ([O I]) cm^{-3}	4×10^6
N_e ([N II]) cm^{-3}	10^4
Excitation class ([O III]/Hβ)	7.5
Excitation class ([He II]/Hβ)	7
A_V (Balmer)	5.75 ± 0.36
A_V (continuum)	7.3

90 000 K yields the relation

$$3 \log r + 2 \log \langle N_e \rangle = 5.20 + 2 \log (R^*/R_\odot),$$

where r is the radius of the Stromgren sphere in pc and $\langle N_e \rangle$ is a mean density representative of the entire nebula. We shall adopt $\langle N_e \rangle = 10^3$ cm^{-3} (since the forbidden lines always sample the densest parts of the nebula), $\log (R^*/R_\odot) = -1.0$ (*cf.* O'Dell 1963), thus $D = 2.3$ kpc (corresponding to an angular size ~10 arcsec). This yields an estimate of the nebular mass of order $0.05 M_\odot$. At this distance in this direction ($l^{II} = 20°$, $b^{II} = -1°$) the interstellar extinction can be as high as 4.7 mag (Fitzgerald 1968), of the same order as the extinction derived from the Balmer decrement.

The nebular continuum predicted from the Balmer emission lines is larger than that observed at all wavelengths, and this problem is not resolved by altering the temperature and electron density. One possible explanation for this could be that the continuum suffers a greater extinction than that of the hydrogen lines; in fact A_V(continuum) ~ 7.3.

3.8 PARSAMYAN 22

This faint bipolar nebula (Parsamyan 1965) containing a seventeenth magnitude central star is well shown by Herbig (1960, his Fig. 12; see also Cohen (1974b) where the object is incorrectly referred to as P 22a). Due to the faintness of the nebula we have concentrated our efforts upon the central star. We classify this as A5 V on the basis of the absorption line profiles of Hβ and Hγ. The shape of the stellar continuum then indicates $A_V = 2.9$.

Herbig (1960) suggests a distance ~1.2 kpc to the dark clouds against which P 22 is projected, on the basis of his estimates of the distance moduli of associated bright stars. In this direction ($l^{II} = 79°$, $b^{II} = 2°$) we expect an interstellar extinction of ~3 mag at 1 kpc distance (*cf.* Fitzgerald 1968). Consequently, all the extinction towards P 22 appears to be interstellar. We have matched an 8500 K blackbody to the de-reddened optical continuum between 4300 and 6700 Å to assess the total stellar luminosity. This amounts to $L^* = 22.4 D^2 L_\odot$, where D is the distance in kpc. Our near-infrared photometry yields additional luminosity $1.0 D^2 L_\odot$ (for $\lambda \geqslant 2.3\ \mu$m). Thus $L_{bol} \geqslant 34 L_\odot$ for P 22.

Our spectra of the star show emission at Hα and weak emission in the core of Hβ. The estimated Balmer decrement indicates that the ionization is produced entirely by collisions in a compact, highly dense envelope, like that surrounding Lk Hα-233 (*cf.* Gerola *et al.* 1971).

3.9 M1–99

This object appears to consist of a sizeable optical nebulosity with two separate components, associated with radio (e.g. Pipher *et al.* 1976) and infrared emission (Allen & Penston 1975; Sibille *et al.* 1975; Pipher *et al.* 1976; CRL 2584 in Price & Walker 1976). We have obtained

optical spectra of the bright condensation within the southern nebulosity that corresponds to object 8 in Table 1 by Pipher *et al.*, and near-infrared photometry of the closest infrared source to this condensation.

Our spectrum of this knot reveals strong Hα, Hβ, Hγ, [N II], [O III] emission lines, weak [O I], and a weak but definite continuum. The Balmer decrement indicates an extinction $A_V = 7.73 \pm 0.12$. After correction for this we find an excitation class of 2.5 based upon the ration of [O III] to Hβ; $T_e \lesssim 8500$ K from the ratio of [N II] lines and, for $T_e = 7500$ K, $N_e \sim 3 \times 10^4$ cm^{-3}; $N_e \lesssim 6 \times 10^5$ cm^{-3} for the [O III] emitting region, adopting $T_e = 7500$ K. The continuum is very red. For $T_e = 7500$ K and $N_e = 3 \times 10^4$ cm^{-3}, the expected continuum due to free–free, bound–free and two-photon processes of hydrogen accounts for only a small fraction of that actually observed. Most of the continuum flux could represent scattered light from a hot star that excites the nebula. Our scanner narrowband indices yield $A_V = 8.2 \pm 1.3$, after allowance for the expected nebular continuum, and assuming the intrinsic colours of an O star.

From the ratio of the observed Hβ flux to the observed continuum at λ 4861 (corrected for nebular processes) we can derive the temperature of the exciting star. We find $T^* = 35\,000$ K, corresponding to an O9 V star (Panagia 1973). It would appear that this star corresponds to one of the compact H II regions and infrared objects observed by Pipher *et al.* (their source 1). However, there is a small displacement between the optical knot and the infrared source that may indicate that radiation is escaping from the embedded star in a direction of reduced nebular density. The match between the extinctions of the Balmer lines and of the stellar continuum suggests that the knot is an integral part of the ionized zone around the O9 star, and that scattering dust particles coexist with ionized gas within this zone. However, this one star is not capable of producing the complex of infrared and radio sources that is apparently associated with M1–99. M1–99 probably represents a nebula expanding away from an embedded cluster of O stars (*cf.* Maucherat 1975; Pipher *et al.* 1976), rather than a bipolar nebula.

3.10 PARSAMYAN 15

This object (Parsamyan 1965) appears to consist of two bright nebulous lobes (Fig. 1) on the Sky Survey photographs. However, a Crossley reflector plate obtained by E. A. Harlan reveals two bright stars within a rather weak nebulosity and shows the presence of a third, very faint star, close to the eastern star. We have obtained optical spectra of these three stars and infrared measurements with a 17 arcsec aperture centred on each (Table 2).

Table 7 presents our spectral classifications, synthesized V and $(B-V)$ data, values of the extinction A_V (based upon both $E(B-V)$ and our scanner narrowband indices) for the three stars in the system. No emission lines occur in the spectra of the brighter stars, but Hα, λ 6300 of [O I] and the λ 5157 nebular line (*cf.* Meinel, Aveni & Stockton 1969) are strong in the spectrum of the faint central object, which is associated with the brightest infrared emission.

Table 7. Parameters for stars in Parsamyan 15.

Star	Spectral type	V	$(B-V)$	A_V
East	A5 V	12.50	0.32	0.56
West	F8 V	13.44	0.68	0.34
Central	A:	18.38	0.98	3:

The distances to the east and west stars are 1.0 and 0.7 kpc, respectively, based upon M_V (from Allen 1973), together with our V and A_V. The distance to the central star apparently exceeds 9 kpc (for an A0 V star), suggesting that there is an appreciable component of neutral extinction or that the star is seen only indirectly. We can predict the 2.3- and 3.5-μm brightness of the stars using Johnson's (1966) mean $(V-K)$ and $(V-L)$ colours of stars. For the west star we predict [2.3] ~ 11.8 and [3.5] ~ 11.6, consistent with the detection and upper limit, respectively. The infrared measurements of the east star are contaminated by the emission of the central source (*cf.* the geometry in Fig. 1 and the data in Table 2). Both these stars are, therefore, foreground objects projected against a rather amorphous nebulosity that surrounds the central star.

The nature of the central star is much less clear. The composite (de-reddened) photometry between 0.4 and 3.5 μm is suggestive of an A star, neutrally extinguished by ~ 3 mag, and an infrared excess that first becomes apparent at 2.3 μm. This excess, at 2.3 and 3.5 μm, could correspond to emission by grains at ~ 700 K. It could represent a young, nebulous, early-type emission-line star embedded in a dust cloud and crossed by a dark lane, rather like the situation for Lk Hα-101 in NGC 1579 (Herbig 1956; Cohen & Woolf 1971).

4 Conclusions

One of the difficulties encountered in constructing an HR diagram that includes all the bipolar nebulae is that each group of investigators has used different methods of analysis for specific nebulae. We have attempted in the present paper to treat the various nebulae consistently when radio, optical and infrared data exist. Fig. 5 presents the HR diagram for 13 bipolar nebulae based upon either the luminosity and temperature given in the present

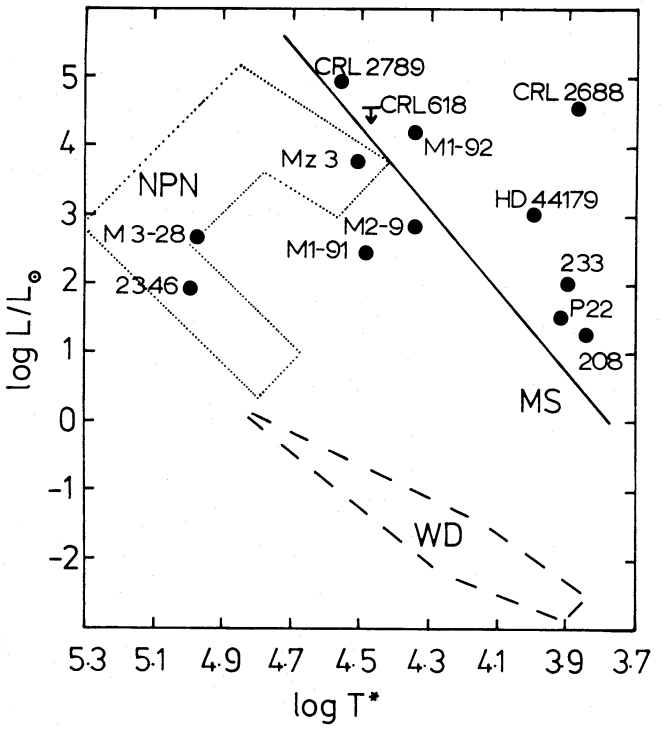

Figure 5. HR diagram for 13 bipolar nebulae. MS represents the main sequence for population I; NPN the Harman–Seaton sequence for the nuclei of planetary nebulae; and WD the region occupied by white dwarfs.

Table 8. Data for the class of bipolar nebulae.

Object	D (kpc)	log ($L_{bol}/L_\odot$)	log T^*
Lk Hα-233	0.88	2.08	3.90
Lk Hα-208	≥0.44	1.30	3.85
M2–9	0.9	2.83	4.34
M1–91	3.1	2.47	4.48
CRL 618	<2.5	<4.57	4.48
NGC 2346	1.7	1.94	5.00
M3–28	2.3	2.76	4.95
P 22	1.2	1.53	3.97
HD 44179	0.4	3.19	4.00
CRL 2688	1.5	4.61	3.86
M1–92	3.0	4.20	4.34
CRL 2789	7.5	4.93	4.56
Mz-3	1.8	3.78	4.51

Note:
All estimates of L_{bol} are lower limits to the total luminosity.

paper, or, for CRL 2789 (Paper III), M1–92 (Paper II) and Mz–3 (Cohen *et al.* 1977; Paper IV) a reanalysis of pre-existing data by the scheme applied above to M2–9 and M1–91. The location of HD 44179 is based upon the data of Paper I but is extremely model dependent (*cf.* Greenstein & Oke 1977). The point plotted for CRL 618 represents an upper limit using the maximal distance of 2.5 kpc discussed by Westbrook *et al.* (1975). Table 8 summarizes these data.

Despite the bipolar nebular structure, M1–99 does not seem to represent the bipolar phenomenon since it contains several exciting stars. Similarly, Parsamyan 15 properly belongs with the nebulous early-type emission-line stars rather than among the bipolars. CRL 2688 is plotted in Fig. 5 but its nature is still very unclear and we shall not discuss it further here (*cf.* Paper II).

4.1 LK Hα-233, LK Hα-208 AND PARSAMYAN 22

These three objects all seem to be associated with dark clouds; all are overluminous for their spectral types; all have late A or early F photospheric spectra with few emission lines; all have collisional ionization of their hydrogen envelopes. Their relatively cool photospheres and the requirement of ionization that is completely due to collisional processes argue strongly for high-velocity stellar winds. Such winds would not be characteristic of stars in immediate post-main sequence phases. Consequently we classify these as objects in pre-main sequence evolution. The nebulae are not ionized but rather reflect the light of the central stars and the hydrogen envelopes. The fading out of the nebula around Lk Hα-208 is particularly suggestive of the progressive weakening of the starlight at increasing distance. Infrared emission by hot dust grains characterizes all three objects and this too is consistent with their being young stars. HD 44179 may also belong to this group of objects.

4.2 M1–92, CRL 2789, MZ-3, M2–9, M1–91 AND CRL 618

These six nebulae are characterized by their isolated nature; none lie in dark clouds or young associations. Their forbidden line spectra are generally indicative of the presence of dense condensations. Thermal emission by dust grains is a common process. These nebulae appear

to consist of quite regular lobes, typically elliptical, which may hold the clue to the process of mass ejection by which they were formed. This morphology suggests that the nebulae are matter bounded, rather than ionization bounded. All have central stars with $T^* \sim 30\,000$ K. The analysis of the data has assumed the mass of a planetary nebula shell and the total ionization of this shell in order to deduce T^* and the distances to these objects. However, their luminosities depend heavily upon the infrared data and this is independent of these assumptions. Their locations in the HR diagram suggest that they belong with the youngest nuclei of planetary nebulae and this argues in part for the self-consistency of our analysis in terms of proto-planetary nebulae.

The emission-line spectra of these objects are quite different from one another and there seems to be a gradation from the presence of strong permitted Fe II lines in the most luminous (CRL 2789, M1–92) to the presence of [Fe III] lines with diminishing intensity in Mz-3, M2–9 and CRL 618. There is also evidence for the existence of high velocity fields (~ 600 km/s) in CRL 2789 and M1–92. It is possible to interpret these two objects as higher mass stars than the other four, in which strong stellar winds are present and in which the nebular spectra arise in regions of predominantly very high density. The dominant [Fe II] and [Fe III] spectra of the other objects suggest that they have much lower density circumstellar envelopes.

4.3 M3–28 AND NGC 2346

These two nebulae contain extremely hot nuclei. They show either spectroscopic and/or photographic evidence for dense condensations, and their ragged edges are suggestive of evolved nuclei whose ability to ionize their nebulae has been diminishing, resulting in recombination of the ionized species in the gas shells.

Acknowledgments

We gratefully acknowledge Drs C. Heiles, L. V. Kuhi, W. M. Fawley and W. Mathews for valuable discussions. We would like to thank D. Myers, C. Sparks, J. Weaver and W. Scharlach for all their assistance with the radio observations at NRAO. The image-tube scanner at Lick Observatory was developed under grant GP-29684 from the National Science Foundation. NC thanks Consejo Nacional de Investigaciones Científicas y Tecnológicas of Venezuela for financial support. MC thanks the National Science Foundation for its support under grant AST75-08513.

References

Allen, C. W., 1973. *Astrophysical quantities,* third edition, University of London Press.
Allen, D. A. & Penston, M. V., 1975. *Mon. Not. R. astr. Soc.*, **172**, 245.
Allen, D. A. & Swings, J. P., 1972. *Astrophys. J.*, **174**, 583.
Aller, L. H., Czyak, S. J., Buerger, E. G. & Lee, P., 1972. *Astrophys. J.*, **172**, 361.
Aller, L. H. & Liller, W., 1968. In *Stars and stellar systems,* eds Middlehurst, B. M. & Aller, L. H., volume VII, p. 483.
Capriotti, E. E., 1964. *Astrophys. J.*, **139**, 225.
Chopinet, M. & Lortet-Zuckerman, M. C., 1976. *Astr. Astrophys. Suppl.*, **25**, 179.
Cohen, M., 1973a. *Mon. Not. R. astr. Soc.*, **161**, 105.
Cohen, M., 1973b. *Mon. Not. R. astr. Soc.*, **164**, 395.
Cohen, M., 1974a. *Mon. Not. R. astr. Soc.*, **169**, 257.
Cohen, M., 1974b. *Publ. astr. Soc. Pacific,* **86**, 813.
Cohen, M., 1977. *Astrophys. J.*, **215**, 533. (Paper III.)

Cohen, M., Anderson, C. M., Cowley, A., Coyne, G. V., Fawley, W. M., Gull, T. R., Harlan, E. A., Herbig, G. H., Holden, F., Hudson, H. S., Jakoubek, R. O., Johnson, H. M., Merrill, K. M., Schiffer, F. H., Soifer, B. T. & Zuckerman, B., 1975. *Astrophys. J.*, **196**, 179. (Paper I.)
Cohen, M. & Barlow, M. J., 1974. *Astrophys. J.*, **193**, 401.
Cohen, M. & Barlow, M. J., 1975. *Astrophys. Lett.*, **16**, 165.
Cohen, M., Fitzgerald, M. P., Kunkel, W., Lasker, B. M. & Osmer, P. C., 1977. *Astrophys. J.*, in press (Paper IV.)
Cohen, M. & Kuhi, L. V., 1976. *Publ. astr. Soc. Pacific*, **88**, 353.
Cohen, M. & Kuhi, L. V., 1977a. *Astrophys. J.*, **213**, 79. (Paper II.)
Cohen, M. & Kuhi, L. V., 1977b. *Mon. Not. R. astr. Soc.*, **180**, 37.
Cohen, M. & Woolf, N. J., 1971. *Astrophys. J.*, **169**, 543.
Fitzgerald, M. P., 1968. *Astr. J.*, **73**, 983.
Gerola, H., Salem, M. & Panagia, N., 1971. *Astrophys. Space Sci.*, **10**, 383.
Greenstein, J. L. & Oke, J. B., 1977. *Publ. astr. Soc. Pacific*, **89**, 131.
Herbig, G. H., 1954. *Astrophys. J.*, **119**, 483.
Herbig, G. H., 1956. *Publ. astr. Soc. Pacific*, **68**, 353.
Herbig, G. H., 1960. *Astrophys. J. Suppl.*, **4**, 337.
Johnson, H. L., 1966. *A. Rev. Astr. Astrophys.*, **4**, 193.
Kaler, J. B., Aller, L. H. & Czyzak, S. J., 1976. *Astrophys. J.*, **203**, 636.
Kazès, I., Le Squéren, A. M. & Gadéa, F., 1975. *Astr. Astrophys.*, **42**, 9.
Kohoutek, L. & Senkbeil, G., 1973. In 18th Liège colloquium: *Les nébuleuses planétaires*, p. 485.
Marsh, K. A., Purton, C. R. & Feldman, P. A., 1976. *Astr. Astrophys.*, **49**, 211.
Maucherat, A. J., 1975. *Astr. Astrophys.*, **45**, 193.
Meinel, A., Aveni, A. & Stockton, M. W., 1969. *Catalog of emission lines in astrophysical objects*, University of Arizona, Tucson, Arizona.
Ney, E. P., Merrill, K. M., Becklin, E. E., Neugebauer, G. & Wynn-Williams, C. G., 1975. *Astrophys. J. Lett.*, **198**, L129.
O'Dell, C. R., 1963. *Astrophys. J.*, **138**, 67.
Osterbrock, D. E., 1974. *Astrophysics of gaseous nebulae*, Freeman, San Francisco.
Panagia, N., 1973. *Astr. J.*, **78**, 929.
Parsamyan, E. S., 1965. *Izv. Akad. Nauk Arm. SSR*, **18**, 146.
Perek, L. & Kohoutek, L., 1967. *Catalogue of galactic planetary nebulae*, Prague.
Pipher, J. L., Sharpless, S., Savedoff, M. P., Kerridge, S. J., Krassner, J., Schurmann, S., Soifer, B. T. & Merrill, K. M., 1976. *Astr. Astrophys.*, **51**, 255.
Purton, C. R., Feldman, P. A. & Marsh, K. A., 1975. *Astrophys. J.*, **195**, 479.
Price, S. D. & Walker, R. G., 1976. *AFGL Four Color Infrared Sky Survey, Environmental Research Papers No. 576.*
Sabbadin, F., 1976. *Astr. Astrophys.*, **52**, 291.
Serkowski, K., Mathewson, D. S. & Ford, N. L., 1975. *Astrophys. J.*, **196**, 261.
Sibille, F., Bergeat, J., Lunel, M. & Kandel, R., 1975. *Astr. Astrophys.*, **40**, 441.
van den Bergh, S., 1974. *Astr. Astrophys.*, **32**, 351.
Westbrook, W. E., Becklin, E. E., Merrill, K. M., Neugebauer, G., Schmidt, M., Willner, S. P. & Wynn-Williams, C. G., 1975. *Astrophys. J.*, **202**, 407.